

# Active damping of the scanner for high-speed atomic force microscopy

Noriyuki Kodera, Hayato Yamashita, and Toshio Ando<sup>a)</sup>

*Department of Physics, Kanazawa University, Kakuma-machi, Kanazawa, 920-1192 Japan*

(Received 30 October 2004; accepted 13 March 2005; published online 26 April 2005)

The scanner that moves the sample stage in three dimensions is a crucial device that limits the imaging rate of atomic force microscopy. This limitation derives mainly from the resonant vibrations of the scanner in the  $z$  direction (the most frequent scanning direction). Resonance originates in the scanner's mechanical structure as well as in the  $z$  piezoactuator itself. We previously demonstrated that the resonance originating in the structure can be minimized by a counterbalancing method. Here we report that the latter resonance from the actuator can be eliminated by an active damping method, with the result the bandwidth of the  $z$  scanner nearly reaches the first resonant frequency (150 kHz) of the  $z$  piezoactuator. © 2005 American Institute of Physics. [DOI: 10.1063/1.1903123]

## I. INTRODUCTION

The atomic force microscope (AFM) is a powerful tool for high-resolution imaging of biological samples on a substrate in aqueous solution. However, the scan speed of the AFMs currently available is too slow to capture the dynamic processes of biological macromolecules in real time. The scan speed is determined by the bandwidth of feedback operator that keeps the tip-sample interaction force constant by moving the sample stage up and down depending on the sample height. Since biological samples are soft and fragile, this feedback operation is indispensable for minimizing the interaction force. In this feedback operation, various devices are involved such as cantilevers, a detector for sensing cantilever deflection, a feedback circuit, a  $z$  scanner that moves the sample stage in the  $z$  direction, and so on. The various efforts made to date have been for the purpose of enhancing feedback speed. Viani *et al.* used small cantilevers with resonant frequencies of 150 kHz to image DNA and GroEL-GroES complexes on mica, in liquid.<sup>1,2</sup> Yet, their frame rate was less than 1/s, because the conventional piezotube scanner they used had a low-resonant frequency in the  $z$  direction. To overcome the low-resonant frequency of conventional sample-stage scanners, Sulcheck *et al.*<sup>3,5</sup> and Rogers *et al.*<sup>4</sup> used a cantilever with an integrated zinc oxide piezoactuator capable of deflecting itself to keep the tip-sample interaction force constant. They achieved a feedback bandwidth (i.e., imaging bandwidth) of 38 kHz and a frame rate of  $\sim 4/s$ .<sup>3</sup> However, the self-actuating cantilever inevitably becomes very stiff, and hence is inappropriate for the imaging of soft samples. Although it was performed not with AFM but rather with near-field scanning optical microscopy, Humphris *et al.* achieved an imaging rate  $> 100$  frames/s, using a scan system that employs the mechanical resonance of an optical fiber probe to address the sample.<sup>6</sup> However, this high-speed is achieved without any feedback operation to keep the probe-sample distance constant. Therefore, this

technique is applicable only to the AFM imaging of hard samples. We optimized all the devices involved in the feedback loop, and were able to produce a high-speed AFM that made it possible in the tapping mode of operation to capture a  $100 \times 100$  pixel image within 80 ms.<sup>7-9</sup>

In enhancing further the imaging rate of our high-speed AFM, the  $z$  scanner is an obvious target for improvement, because it is the slowest device among those contained in the feedback loop. The resonant vibrations of the  $z$  scanner are the cause for the slowing of feedback. Resonance due to the scanner's overall structure usually occurs at a frequency lower than the resonant frequency of the  $z$  piezoactuator itself. This structural resonance can be minimized by suppressing the impulsive forces produced when the  $z$  actuator displaces very quickly. As demonstrated previously, this suppression can be made using two  $z$  piezoactuators placed in the opposite direction to one another. The impulsive forces produced by one  $z$  actuator are countered by the simultaneous displacement of the other  $z$  actuator of the same length, in the counter direction.<sup>7</sup> The challenge is to damp completely the resonant vibrations of the  $z$  piezoactuators themselves. A conventional method uses a notch filter to remove a frequency band around the resonant frequency. A weak point of this method is the slow transient response of the notch filter. In this article, we show that excellent damping can be accomplished by a method of active vibration control of the  $z$  actuators. Because the quality factor ( $Q$ ) of the  $z$  actuators' resonance is markedly reduced by this method, the response speed is greatly enhanced. Although the phase delay is pronounced with this active damping, it can be compensated by means of an inverse transform function method. Together with this compensation, the  $z$  scanner can operate from dc up to a high frequency that exceeds its first resonance frequency, without considerable phase delay.

## II. EXPERIMENTS

### A. Apparatus

The home-made high-speed AFM apparatus used here is basically the same as reported previously.<sup>7</sup> The  $z$  scanner has

<sup>a)</sup>Electronic address: tando@kenroku.kanazawa-u.ac.jp

two piezoactuators placed in the opposite direction to one another. The  $z$  piezoactuators are replaced with customized stack piezoactuators ( $3 \times 3 \times 3 \text{ mm}^3$ , NEC-Tokin, Tokyo) with the self-resonance frequency of 420 kHz and a maximum displacement of 900 nm (at 100 V). A sample stage, which is a glass of a circular-trapezoid shape with a small top surface of 1 mm diameter, is attached onto the top of one of the  $z$  actuators via a thin layer of vacuum grease. To maintain balance, a dummy stage that has the same mass as the sample stage is attached to the other  $z$  piezoactuator. The amplifier (M-2331, Mess-Tek. Corp., Saitama, Japan) can drive the  $z$  piezoactuator (22 nF) at up to 1 MHz. A cantilever tip is in contact with the sample stage surface in order to monitor displacement of the  $z$  actuator. The cantilever is immersed in water, to overcome the problem of the slow response in air due to the high  $Q$  value ( $\sim 200$ ). The cantilever deflection is detected with an optical system whose design was reported previously.<sup>7</sup> These cantilevers are recently developed ones from Olympus; the resonant frequency is  $\sim 800$  kHz in water, and the spring constant is  $\sim 100$  pN/nm.<sup>10</sup> The cantilever tip is further extended by electron beam deposition. The open-loop transfer functions of the  $z$  scanner and the entire closed loop transfer functions are measured with a frequency analyzer (FRA-5096, NF Corp., Yokohama). Since the resonance frequency of the cantilever is approximately 800 kHz in water, reliable measurements of displacement of the  $z$  scanner are limited to frequencies less than  $\sim 500$  kHz.

### B. Active damping of $z$ piezovibrations

The open-loop transfer function of the  $z$  scanner is represented by curves (a) in Fig. 1. A resonant peak appears around 150 kHz, with  $Q=18$ . A tiny bump in the gain which appears around 50 kHz is due to structural resonance of the  $z$  scanner. Without counter-balancing [curves (b)], it appears with a much larger amplitude. Active  $Q$  control of cantilever vibration has recently been used for various purposes, such as sensitizing the tip-sample interaction by increasing  $Q$ ,<sup>11,12</sup> or enhancing the cantilever's response speed by decreasing  $Q$ .<sup>13,14</sup> This technique can be applied to any resonant system. The output signal from the resonant system to be controlled is phase shifted by  $\pm 90^\circ$ , and its gain-controlled signal is added to the signal that drives the system. This addition results in a change in the apparent viscous drag force, and hence enhances or reduces the system's  $Q$ . When this technique is applied to the  $z$  actuators, it is necessary to detect the displacement of the  $z$  actuators, which is not easy to do.

The mechanical response of the  $z$  actuators is well approximated by a second-order transfer function

$$G_{\text{piezo}}(s) = \frac{K\omega_p^2}{s^2 + (\omega_p/Q_p)s + \omega_p^2}, \quad (1)$$

where  $\omega_p = 2\pi f_p$ ,  $f_p$  is the resonance frequency of the  $z$  piezo,  $Q_p$  is the quality factor of the  $z$  piezo's resonant vibration, and  $K$  is the ratio of the static displacement to the voltage applied to the piezo. The input-output relationship is determined only by the transfer function, and is independent of the other physical properties. Therefore, instead of monitor-

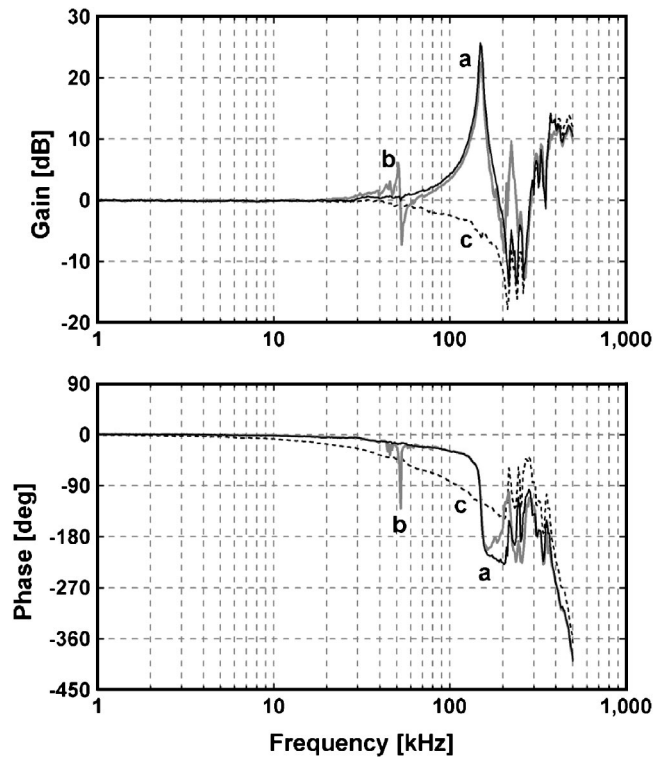


FIG. 1. Open loop transfer functions of the  $z$  scanner. (a) Without active damping and with counter balancing, (b) without active damping and counter balancing, and (c) with active damping and counter balancing.

ing displacements of the each  $z$  piezoactuator, it is possible to monitor output signals from a resonant system (“mock”  $z$  actuator) which is characterized with the same transfer function as that of the  $z$  piezo-actuator. We constructed the mock actuator from a  $LCR$  circuit that was tuned to have  $1/\sqrt{LC} = \omega_p$  and  $\sqrt{L/R^2C} = Q_p$ . The resonance frequency and  $Q$  were adjusted with a variable capacitor and a variable resistor, respectively. Figure 2 is the block diagram that was used in the active damping control design. The driving signal [proportional-integral-differential (PID) output when operated with a feedback loop] was branched into two signals to control separately the  $z$  piezo for the sample stage displacement and the  $z'$  piezo for the counterbalancing. The output signals from the mock  $z$  and  $z'$  actuators were phase shifted by  $-90^\circ$  to reduce their  $Q$  values, which eventually reduced the natural  $Q$  values ( $=18$ ) of the real  $z$  and  $z'$  piezoactuators down to  $1/2$ . As shown in Fig. 1 [curve (c) in the upper panel], the resonance completely disappeared as a result of this active damping. In addition, the transient response speed of the  $z$  scanner was markedly increased, as shown in Fig. 3. In this measurement, the  $z$  scanner was started at  $t=150 \mu\text{s}$ , driven by sinusoidal ac signals with a frequency of 150 kHz. Without active damping [Fig. 3(a)], the  $z$  scanner responded slowly with a settling time of about  $38 \mu\text{s}$ , while with active damping [Fig. 3(b)] it responded very quickly with a settling time of about  $1.1 \mu\text{s}$ . These settling times ( $\tau$ ) coincided with the expectation derived from the relationship of  $\tau = Q/\pi f_p$ .

### C. Inverse transfer function compensation

However, a drawback is that the phase delay became pronounced as shown in Fig. 1 (lower panel); the frequency

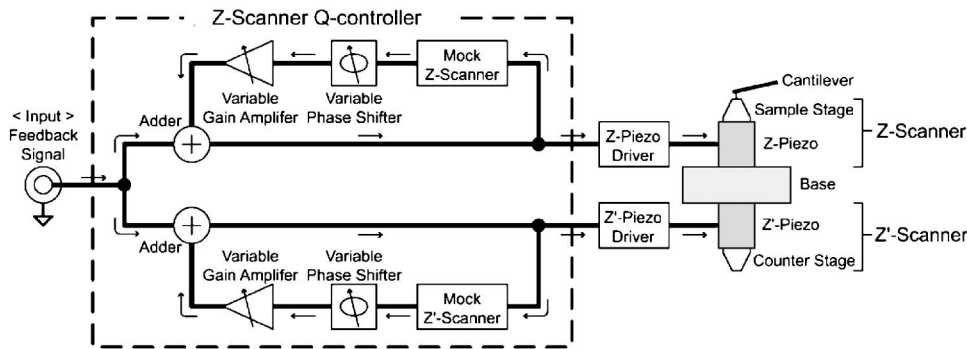


FIG. 2. Schematic diagram for the active damping control. The input signal is the output from the PID controller, when the feedback operation is made. The  $z$  and  $z'$  piezoactuators are separately controlled. When the phase compensation is made, the circuits of one PD or two PDs in series with notch filters in series (for removing noise with frequencies higher than 1 MHz) are placed just after the input signal.

that gives a  $45^\circ$  phase delay was lowered from 132 to 51 kHz. At  $Q=1/2$ , the transfer function [Eq. (1)] becomes

$$G_{\text{piezo}}(s) = \frac{K}{(1 + s/\omega_p)^2}. \quad (2)$$

Therefore, the phase delay can be compensated with an inverse transfer function, i.e.,

$$G(s) = K'(1 + s/\omega_p)^2. \quad (3)$$

This inverse transfer function can be constructed by two PD controllers in series, one of which can be left to the original PID controller when operated in the closed feedback loop.

Figure 4 shows the compensation effect of the two PD controllers in series. As a result of the compensation the frequency at the  $45^\circ$  phase delay is extended from 51 to 131 kHz, and the gain became nearly even at up to 180 kHz. However, because the phase compensation increases the gain in proportion to the frequency, higher-order resonant vibrations were increased. We solved this problem using additional active damping controllers with mock actuators having small  $Q$ 's to suppress vibrations at the higher frequencies ( $<1$  MHz). The remaining high-frequency noise ( $>1$  MHz) that enters the piezodrive amplifier was removed by notch filters in series. Because the frequency band eliminated by the notch filters is far from the first resonant frequency of the real piezoactuators, the phase delay around the first resonant frequency was not significantly promoted by the filters. Figure 5 compares the whole closed-loop transfer functions of the  $z$  scanner with and without the active damping. In this measurement the set-point voltage of the PID circuit was varied by means of sinusoidal signals, and the

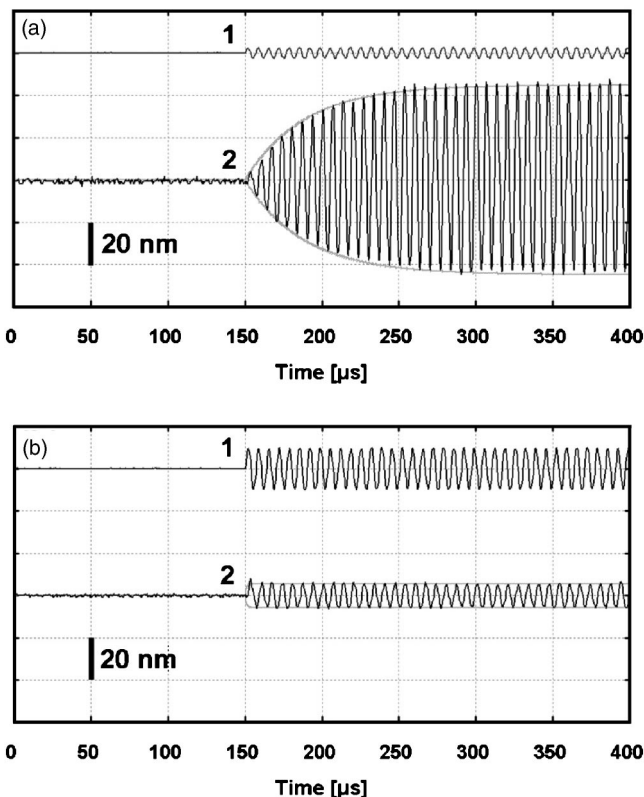


FIG. 3. Effect of active damping on the transient response of the  $z$  scanner. In (a), the  $z$  scanner has its natural  $Q(=18)$ , while in (b) the  $z$  scanner is actively damped so that its  $Q$  is reduced to 0.5. The  $z$  scanner began to oscillate at  $t=150 \mu\text{s}$  by ac signals (lines "1") of 150 kHz. The amplitude of the ac input signals was attenuated when operated without active damping. The enveloping curves (gray lines) of the  $z$  scanner's displacements (lines "2") indicate the transient changes in the amplitude of the  $z$ -scanner's oscillation.

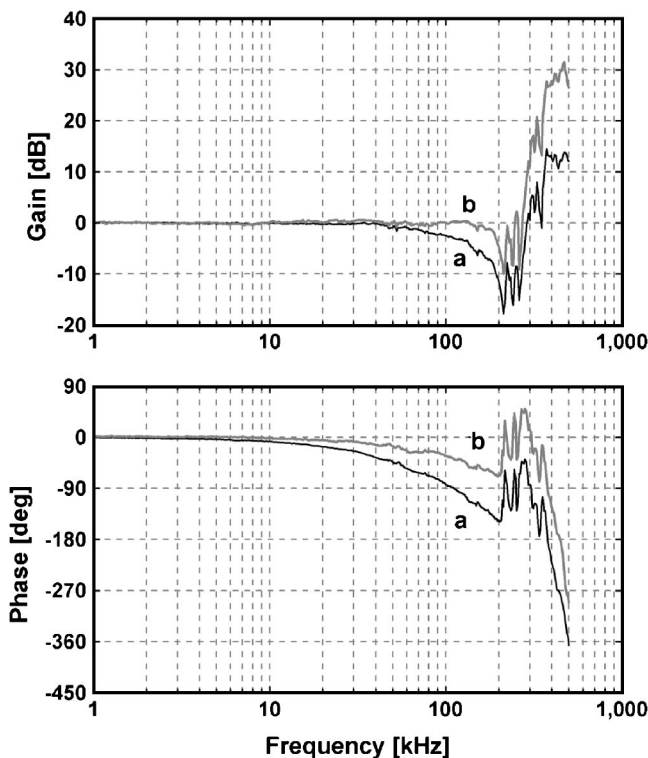


FIG. 4. Open-loop transfer functions of the actively damped  $z$  scanner obtained without phase compensation (a) and with phase compensation (b).

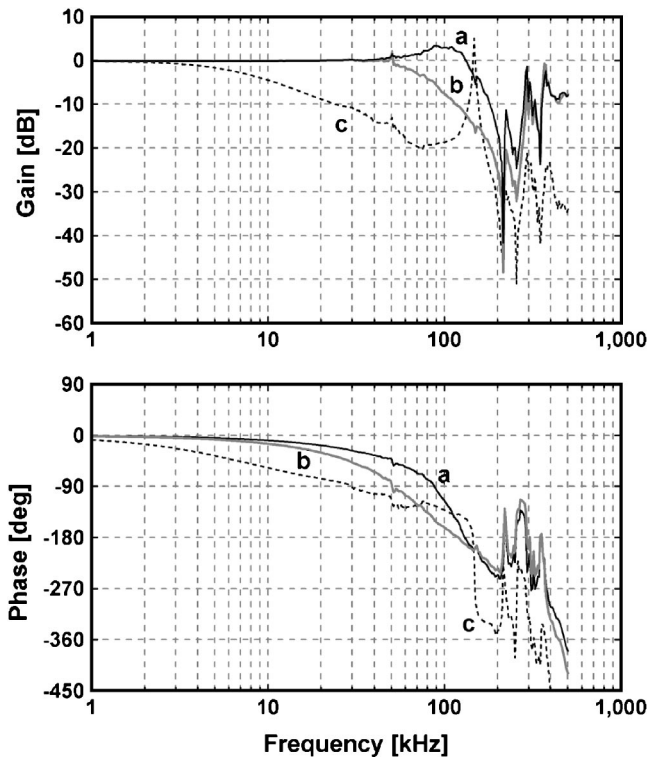


FIG. 5. Closed-loop transfer functions. While the set point of the PID controller is being perturbed, the cantilever deflection is monitored. The transfer functions are obtained with active damping and phase compensation (a), with active damping without phase compensation (b), and without active damping (c).

resulting cantilever deflection signals were monitored. In each measurement of the transfer function, the parameters of the PID controller were adjusted to achieve the best feedback condition. The feedback bandwidth (defined as the frequency at the  $45^\circ$  phase delay) was 7 kHz without the active damping. With active damping, the bandwidth was increased to 29 kHz, and increased further to 50 kHz with the additional effect of the phase compensation with one PD controller. Figure 6 depicts the difference in the feedback bandwidths. The pseudo-AFM images [Figs. 6(a) and 6(c)] were constructed from the cantilever's deflection signals that responded to the rectangular variations of the set-point level (corresponding to a 50 nm height change). Figures 6(b) and 6(d) show the image profiles along the time axis, together with the input rectangular signals. Without active damping the response was very slow, so that the rectangular shape was largely distorted. With active damping and phase compensation, the input rectangular signals were well restored in the cantilever's deflection signals.

#### D. Imaging of myosin V in solution

The better performance of the actively damped  $z$  scanner was further demonstrated by images of a real soft sample (myosin V molecules) being captured. The sample was prepared in the same way as described before.<sup>7</sup> Figure 7 shows images captured successively at 21 frames/s, with the scan size of  $240 \text{ nm}$ .<sup>17</sup> Although it is hard to see from the six successive still images of Fig. 7, rapid Brownian movement of the coiled-coil tail region and the tail end was clearly seen

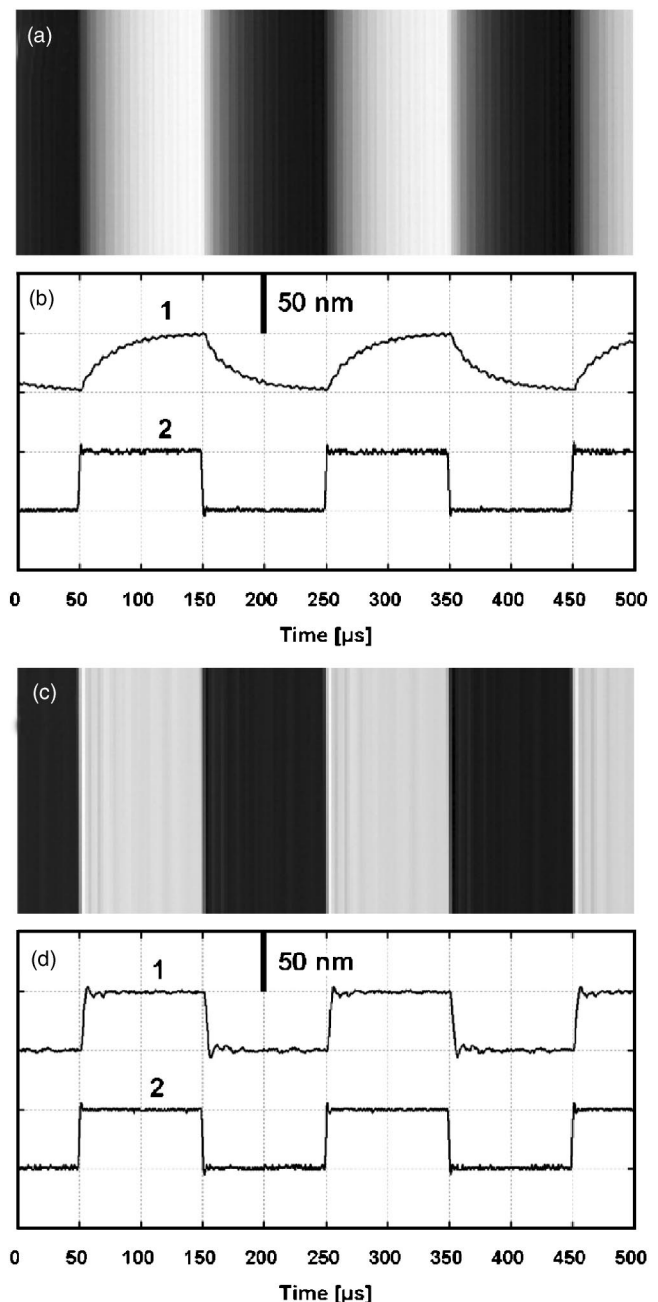


FIG. 6. Response of cantilever deflection signal to rectangular variations of the set point of the PID controller. The upper panels (a), (b) are obtained without active damping of the  $z$ -scanner vibrations, while the lower panels (c), (d) are obtained with active damping. In (a) and (c), pseudo-AFM images constructed from the cantilever deflection signals are shown. In (b) and (d), cantilever deflection signals (lines "1") are shown, together with the rectangular perturbation signals (lines "2").

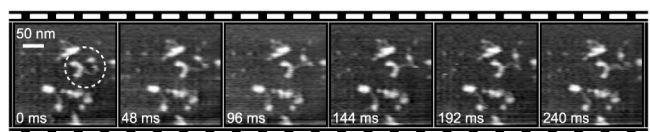


FIG. 7. Successive images of myosin V on mica in buffer solution. The same area of  $240 \times 240 \text{ nm}^2$  was imaged 300 times with  $100 \times 100$  pixels. Only six successive images are shown. The tip speed is  $1 \text{ mm/s}$ , and the frame rate is  $21/\text{s}$ . A typical "Y shaped" myosin V molecule is circled in the first image.

with noises less than those appeared in the images taken before (see Fig. 5 in Ref. 7). Compared with the extensive improvement of the  $z$  scanner, the imaging rate could not be enhanced greatly (only about 1.7 times). A higher imaging rate resulted in the appearance of large periodic noises due to the mechanical vibrations of the sample stage, and in occasional detachment of the cantilever tip from the sample surface. This is because the other elements such as the  $x$  scanner, cantilevers, and electric devices are not improved yet.

### III. DISCUSSION

High-speed AFM imaging has been long sought, especially in the biological sciences, to allow study of the dynamic behavior of biological macromolecules at work. The most problematical device in the quest for fast imaging has proven to be the  $z$  scanner. The resonant vibrations in the  $z$  direction that derive from the scanner's overall structure can be erased by the counterbalancing method.<sup>7</sup> Therefore, an improvement that remains to be made is to increase the resonant frequency of the  $z$  piezoactuator itself. However, the currently available piezoactuators are quite limited. To overcome this obstacle, an active damping system with mock actuators was developed. This is quite a simple system compared to the systems in which displacements of the real piezo-actuators are directly monitored by methods such as capacitance detection or optical detection. Electric charges supplied to the piezo-actuator as well as electric charges induced on the piezoend surfaces are supposed to be proportional to the piezo displacement.<sup>15,16</sup> These charges can be measured by a charge amplifier. Similar to the method we developed here, this method has the advantage that the mechanical design of the scanner does not need to be changed. However, the piezo-actuator as a capacitor couples electrically with the inductor and resistor elements of the actuator, and they form an electrically resonant system. This resonant frequency is usually higher than the mechanical resonant frequency. However, when these frequencies are not markedly different, the charge measurement (as an index of the piezo-displacement) is disturbed by the electrical resonance.

The  $z$  scanner has generally been recognized as the slowest device among those involved in the feedback loop in the tapping mode of the AFM operation. Here, we have found a way to successfully overcome this issue. The bandwidth of the  $z$  scanner now reaches 131 kHz. When a cantilever tip is scanning in the  $x$  direction over a sample with a periodicity of  $\lambda$  at a speed of  $V_s$ , the cantilever oscillation amplitude is modulated at a frequency of  $f_m (=V_s/\lambda)$ . Therefore, the  $z$  scanner has to move at  $f_m$ . From this relationship, the wide bandwidth (131 kHz) achieves scan speeds of up to 1.3 mm/s for samples with an apparent feature of 10 nm. The  $z$  scanner is not the slowest device any longer. Which

device is now the slowest one? We think that it is the cantilevers. In the tapping mode AFM, the bandwidth of the whole feedback loop cannot exceed one eighth of the cantilever resonant frequency ( $f_c$ ) in water. Even when the cantilever oscillation amplitude is read at the fastest speed (as we have done in practice), i.e., at every period of the oscillation, this reading results in a phase delay of  $360^\circ \times f_m/f_c$ , over the amplitude modulation. This phase delay should not exceed  $45^\circ$ , and hence  $f_m$  cannot exceed  $f_c/8$ . This means that the feedback bandwidth will never be able to exceed  $f_c/8$ . The resonant frequency of our tiny cantilevers is about 800 kHz in water, and hence the whole feedback bandwidth cannot exceed 100 kHz, which is narrower than that of the  $z$  scanner.

### ACKNOWLEDGMENTS

This work was supported by CREST/JST, Special Coordination Funds for Promoting Science and Technology (Effective Promotion of Joint Research with Industry, Academia and Government) from JST, and Grant-in-Aid for Basic Research (S) from the Ministry of Education, Sports, Science and Technology of Japan.

- <sup>1</sup>M. B. Viani, T. E. Schäffer, G. T. Palocz, L. I. Pietrasanta, B. L. Smith, J. B. Thompson, M. Rief, H. E. Gaub, K. W. Plaxco, A. N. Cleland, H. G. Hansma, and P. K. Hansma, *Rev. Sci. Instrum.* **70**, 4300 (1999).
- <sup>2</sup>M. B. Viani, L. I. Pietrasanta, J. B. Thompson, A. Chand, I. C. Gebeshuber, J. H. Kindt, M. Richter, H. G. Hansma, and P. K. Hansma, *Nat. Struct. Biol.* **7**, 644 (2000).
- <sup>3</sup>T. Sulchek, R. Hsieh, J. D. Adams, S. C. Minne, C. F. Quate, and D. M. Adderton, *Rev. Sci. Instrum.* **71**, 2097 (2000).
- <sup>4</sup>B. Rogers, T. Sulchek, K. Murray, D. York, M. Jones, L. Manning, S. Malekos, B. Beneschott, J. D. Adams, H. Cavaozs, and S. C. Minne, *Rev. Sci. Instrum.* **75**, 4683 (2003).
- <sup>5</sup>T. Sulchek, G. G. Yaralioglu, C. F. Quate, and S. C. Minne, *Rev. Sci. Instrum.* **73**, 2928 (2002).
- <sup>6</sup>A. D. L. Humphris, J. K. Hobbs, and M. J. Miles, *Appl. Phys. Lett.* **83**, 6 (2003).
- <sup>7</sup>T. Ando, N. Kodera, E. Takai, D. Maruyama, K. Saito, and A. Toda, *Proc. Natl. Acad. Sci. U.S.A.* **98**, 12468 (2001).
- <sup>8</sup>T. Ando, N. Kodera, D. Maruyama, E. Takai, K. Saito, and A. Toda, *Jpn. J. Appl. Phys., Part 1* **41**, 4851 (2002).
- <sup>9</sup>T. Ando, N. Kodera, Y. Naito, T. Kinoshita, K. Furuta, and Y. Y. Toyoshima, *Chem. Phys. Chem.* **4**, 1196 (2003).
- <sup>10</sup>M. Kitazawa, K. Shiotani, and A. Toda, *Jpn. J. Appl. Phys., Part 1* **42**, 4844 (2003).
- <sup>11</sup>B. Anczykowski, J. P. Cleveland, D. Kruger, V. Elings, and H. Fuchs, *Appl. Phys. A: Mater. Sci. Process.* **66**, 885 (1998).
- <sup>12</sup>J. Tamayo, A. D. L. Humphris, A. M. Malloy, and M. J. Miles, *Ultramicroscopy* **86**, 167 (2001).
- <sup>13</sup>T. Sulchek, R. Hsieh, J. D. Adams, G. G. Yaralioglu, S. C. Minne, C. F. Quate, J. P. Cleveland, A. Atalar, and D. M. Adderton, *Appl. Phys. Lett.* **76**, 1473 (2000).
- <sup>14</sup>M. Antognozzi, M. D. Szczelkun, A. D. L. Humphris, and M. J. Miles, *Appl. Phys. Lett.* **82**, 2761 (2003).
- <sup>15</sup>C. V. Newcomb and I. Flinn, *Electron. Lett.* **18**, 442 (1982).
- <sup>16</sup>K. Furutani, M. Urushibata, and N. Mohri, *Nanotechnol.* **9**, 93 (1998).
- <sup>17</sup>See movies placed at the website of [www.s.kanazawa-u.ac.jp/phys/biophys/rsi.htm](http://www.s.kanazawa-u.ac.jp/phys/biophys/rsi.htm)